International Journal of Optomechatronics

ISSN: 1559-9612 (Print) 1559-9620 (Online) Journal homepage: www.tandfonline.com/journals/uopt20

Reconfigurable metamaterials for optoelectronic applications

Yu-Sheng Lin & Zefeng Xu

To cite this article: Yu-Sheng Lin & Zefeng Xu (2020) Reconfigurable metamaterials for optoelectronic applications, International Journal of Optomechatronics, 14:1, 78-93, DOI: 10.1080/15599612.2020.1834655

To link to this article: https://doi.org/10.1080/15599612.2020.1834655

INTERNATIONAL JOURNAL OF OPTOMECHATRONICS
2020, VOL. 14, NO. 1, 78–93
https://doi.org/10.1080/15599612.2020.1834655

Reconfigurable metamaterials for optoelectronic applications

Yu-Sheng Lin and Zefeng Xu

State Key Laboratory of Optoelectronic Materials and Technologies, School of Electronics and Information Technology, Sun Yat-Sen University, Guangzhou, P. R. China

ABSTRACT

In recent years, electromagnetic characteristics of metamaterials has aroused great interest because of innovative fundamental understanding as well as promising potential applications in optics, semiconductors, imaging, and sensing. We survey the state-of-the-art of spatially reconfigurable metamaterials in which electromagnetic Lorentz, Coulomb, and Ampere forces, as well as optical signals and thermal stimulation can be dynamically changed their optical properties. Electro-mechanical and optical inputs change the amplitude, phase, polarization of incident electromagnetic wave, and optical response within these metamaterials, which can be driven by electric or optical signals. Based on a solid theoretical foundation, we review the most recent experimental works on reconfigurable metamaterials endowed with an active tuning characteristic. Additionally, we review the potential metamaterial applications that may inspire new research works and offer a comparison to other optoelectronic fields.

KEYWORDS

Metamaterial; reconfiguration; MEMS; optics; metasurface

1. Introduction

Metamaterial (MM) is a composite material with artificially periodic array structure, which exhibits extraordinary optical properties that cannot found in nature.[1] It can be effectively and easily controlled the amplitude, direction, polarization, wavelength, and phase of incident electromagnetic wave owing to its unique electromagnetic characteristics, such as fano-resonance, negative index, plasmonic resonance, and perfect absorption, electromagnetic-induced transparency effect through the artificial self-constructed periodic configuration.[2] In addition, metamaterials can be applied for electro-optical conversion devices by adjusting the geometrical parameters of metamaterials according to the theory of optical transformation,[3] which can span ultrabroad spectrum range from microwave to ultraviolet light. To compare the traditional nature materials, metamaterials have unprecedented advantages, such as extremely high expansibility and ultrathin characteristics. Therefore, it greatly optimizes many classical devices. For example, optical switches, resonators, waveguides, and filters.[4,5]

Recently, there have been proposed many actively tuning methods by the worldwide researchers. Reconfigurable metamaterial has become a research hotspot in optics, since precise optical control has been possible and come across future applications. Figure 1 shows the roadmap of reconfigurable metamaterials in recent 10 years. The natural frequency of materials has achieved in the way of the scalability of spectrum. The actively tuning and driving methods have been

CONTACT Yu-Sheng Lin linyoush@mail.sysu.edu.cn State Key Laboratory of Optoelectronic Materials and Technologies, School of Electronics and Information Technology, Sun Yat-Sen University, Guangzhou, P. R. China.
This article has been republished with minor changes. These changes do not impact the academic content of the article.

Nomenclature

SRR	split-ring resonator	PEG	polyethylenediformate ethylene glycol
MEMS	micro-electro-mechanical system	LC	inductance–capacitance
Qfactor	quality factor	VO_2	vanadium dioxide
THz	terahertz	CRR	closed ring resonator
IR	infrared	PSM	parabolic-shaped metamaterialparabolic-shaped metamaterial
Si	silicon		
GaAs	gallium arsenide	$LiNbO_3$	lithium niobate
Ge	germanium	FWHM	full width at half maximum
PDMS	polydimethylsiloxane	HEMT	high electron mobility transistor

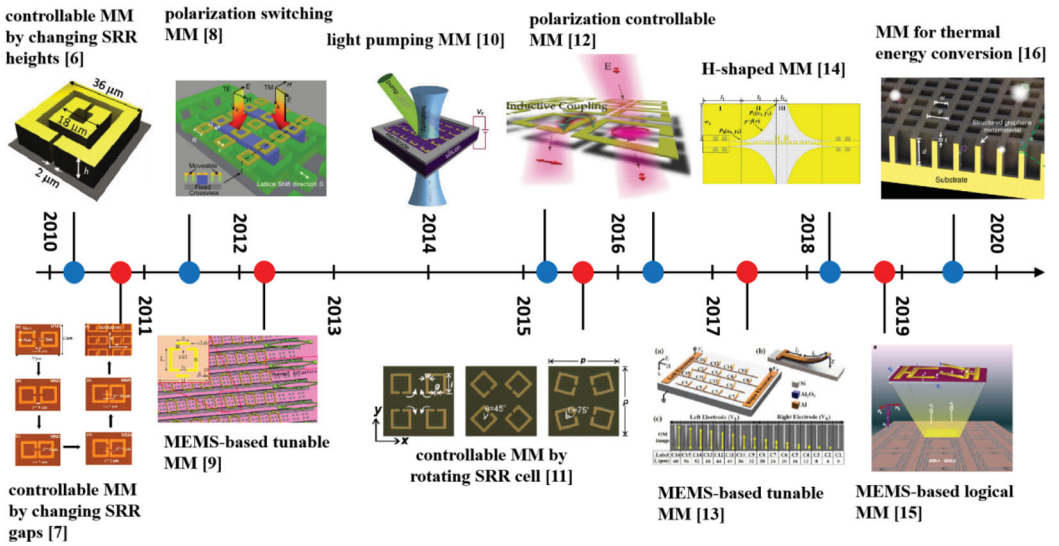

Figure 1. The roadmap of reconfigurable metamaterials in recent 10 years.

introduced into increasing the flexibility and applicability. In 2010, the resonant frequency of electromagnetic metamaterial could be only tuned by changing the geometrical parameters of metamaterial unit cell. For example, Chiam et al. proposed the adjustable metamaterial by changing the dielectric aspect ratio of metamaterial structure.[6] Chowdhury et al. proposed the adjustable metamaterial using split-ring resonator (SRR) configuration by changing the position of SRR gap.[7] In the following years, the emergence of new driving methods made metamaterials more controllable. In 2011, micro-electro-mechanical system (MEMS) technique is proposed to move the metamaterial frame using comb driver by Zhu et al., thus, the polarization characteristic of incident light could be switched.[8] Xiuhan Li et al. proposed continuously tunable metamaterials using MetalMUMPS process in 2012.[9] Quan Li et al. proposed a method using continuous laser pumping and driving voltage simultaneously to perform the dual-tuned metamaterials.[10] In 2015, Al-Naib et al. proposed metamaterial-based SRR with different quality factor (Q-factor) and amplitude depth of resonance by changing the mutual rotation angle between SRRs.[11] Since then, researchers have discovered more methods to actively control the combination of physical electromagnetic effects. Cong et al. proposed the polarization state of incident electromagnetic wave can be tuned by different incident angle and near-field inductive coupling induction.[12] In 2018, Gao et al. proposed a highly selective metamaterial to be a broad bandpass filter using non-periodic surface plasmon polariton.[13] In the meantime, Lee et al. demonstrated MEMS-based

Table 1. Tunable metamaterials using different substrate materials.

Substrates	Features	Applications	Refractive Index	Working Frequency	Reference
Si	1. Large scale 2. Low cost, low loss 3. Easily processed 4. Hard	Wireless strain sensor (2009) Electro-thermal actuator (2014)	3.41–3.52	IR, THz	[33] [34]
GaAs	1. High absorption coefficient 2. Wide frequency-shift and amplitude-shift 3. Hard	THz imaging absorber (2008) THz phase shifter (2006)	3.28–3.41	IR, THz	[35] [36]
Sapphire	1. Low loss (at low temperature) 2. Electromagnetically induced transparency 3. Hard	Optical switch with low loss (2010) near-field Optical resonator (2015)	1.762–1.770	VL	[37] [38]
Ge	1. High absorption 2. Low loss 3. Hard	multi-frequency band absorber (2013)	3.94–4.04	IR	[39]
Quartz	1. Low cost 2. Easily processed 3. Low loss 4. Hard	THz filter (2014) THz resonator (2014)	1.30–1.70	VL, THz	[40] [41]
Polymide	1. High and ultra-low temperature resistance 2. Good mechanical properties 3. Good chemical stability 4. Low dielectric loss 5. Flexible 6. Biocompatibility	High refractive index device (2011) Ultra-thin THz absorber (2015)	1.590–1.592	IR, THz	[42] [43]
Parylene	1. Electromagnetic response 2. Low loss 3. Biocompatibility	Medical imaging (2010)	1.51–1.62	THz	[44]
PDMS	1. Low cost 2. Easy adhesion with si 3. Flexible 4. widely applied in microfluidics field	Stretchable device (2013) Biaxial strain sensor (2013)	1.4–1.45	VL, THz	[45] [46]
PEG	1. Passive tunability 2. Better for 3d metamaterial 3. Complicated process	Refractive Index Meter (2012) Band-stop filter (2014)	1.45–1.46	IR	[47] [48]
Polyester	1. Good thermoplasticity 2. Good compatibility with fluid, e.g. Liquid crystal 3. Good elasticity	THz resonator (2013)	1.53–1.54	THz	[49]

metamaterials to assist the control of incident electromagnetic wave.[14] In 2019, the same research group (Lee et al.) demonstrated two independent SRRs to form the double-cantilevers, which lifting height can be regulated by driving voltage. Thus, the multi-input–output state of metamaterial can be used for the logical operation in the terahertz (THz) frequency range.[15] In 2020, Lin et al. designed a three-dimensional structured graphene metamaterial to achieve omni-directional solar thermal energy conversion.[16] There are also many corresponding reconfigurable metamaterial breakthroughs[17–32] in this decade apart from these relatively milestone research developments.

As reconfigurable metamaterials in optoelectronic applications have progressed rapidly in the past decade, we reviewed the current reconfigurable metamaterials and divided them by different substrates, materials, configurations, and tuning mechanisms spanned from visible, infrared (IR) to THz spectra ranges, and then discussed their potential applications in biosensors, opto-logic operations, and optical communication systems subsequently.

Table 2. Tunable metamaterials using different coupling materials.

Materials	Features	Applications	Refractive Index	Working Frequency	Reference
Metal	1. Popular material for metamaterial construction 2. High electrical conductivity 3. Possible for integration with current ic process 4. Obvious lc resonance	Ultra-sensitive THz sensor (2014) Thin-film sensor (2010) Protein sensor (2017) Plasma photoconductive antenna (2019)	1.0–10.0	VL, IR, THz	[50] [6] [51] [52]
Semiconductor	1. Tunable conductivity and inductance 2. Light excitation 3. changeable dielectric constant and carrier density 4. Possible for integration with current ic process	Dynamic trap filter (2008)	1.0–5.0	VL, IR, THz	[53]
Phase-change material	1. Phase transitions triggered by electricity, heat or light 2. Large absorption 3. Temperature-sensitive	Tunable absorber (2019)	1.0–2.0	VL, IR, THz	[54]
Superconducting material	1. Negative refractive index 2. Anti-magnetic 3. High conductivity 4. Low loss	High temperature superconducting film (2010) Antireflection film (2010)	0.1–5.0	VL, IR, THz	[55] [56]
Graphene	1. Large absorption bandwidth 2. Good mechanical toughness 3. High electron mobility	Broadband absorber (2017) Broadband THz polarization converter (2018)	4.3–4.6	VL, IR, THz	[57] [58]

2. Basic elements of reconfigurable metamaterials

2.1. Substrates

The substrate is an important element of reconfigurable metamaterials that directly determines the optical performance. Since geometrical size of substrate is generally much larger than that of metamaterials, its essential property restricts the flexibility and adaptability in the real applications. As the research progresses, there are many kinds of substrates introduced to apply in different application scenarios. It is considering the flexible and rigid characteristics. They are divided into hard materials, e.g. silicon (Si),[33,34] gallium arsenide (GaAs),[35,36] sapphire,[37,38] germanium (Ge),[39] quartz,[40,41] and flexible materials, e.g. polyimide,[42,43] parylene,[44] polydimethylsiloxane (PDMS),[45,46] polyethylenediformate ethylene glycol (PEG),[47,48] polyester.[49] The relative features and applications are summarized in Table 1.

2.2. Materials

The reconfigurable metamaterial is a broad concept. It can be defined that their electromagnetic properties of metamaterials can be tuned. The material is the key element of reconfigurable metamaterial to determine the required electromagnetic characteristics. The commonly used materials are with special optical properties, such as Au, semiconductors, and graphene. The typical materials used in the reconfigurable metamaterial researches, including metallic materials,[6,50–52] semiconductor materials,[53] phase-change materials,[54] superconducting materials,[55,56] and graphene.[57,58] The relative features and applications are summarized in Table 2.

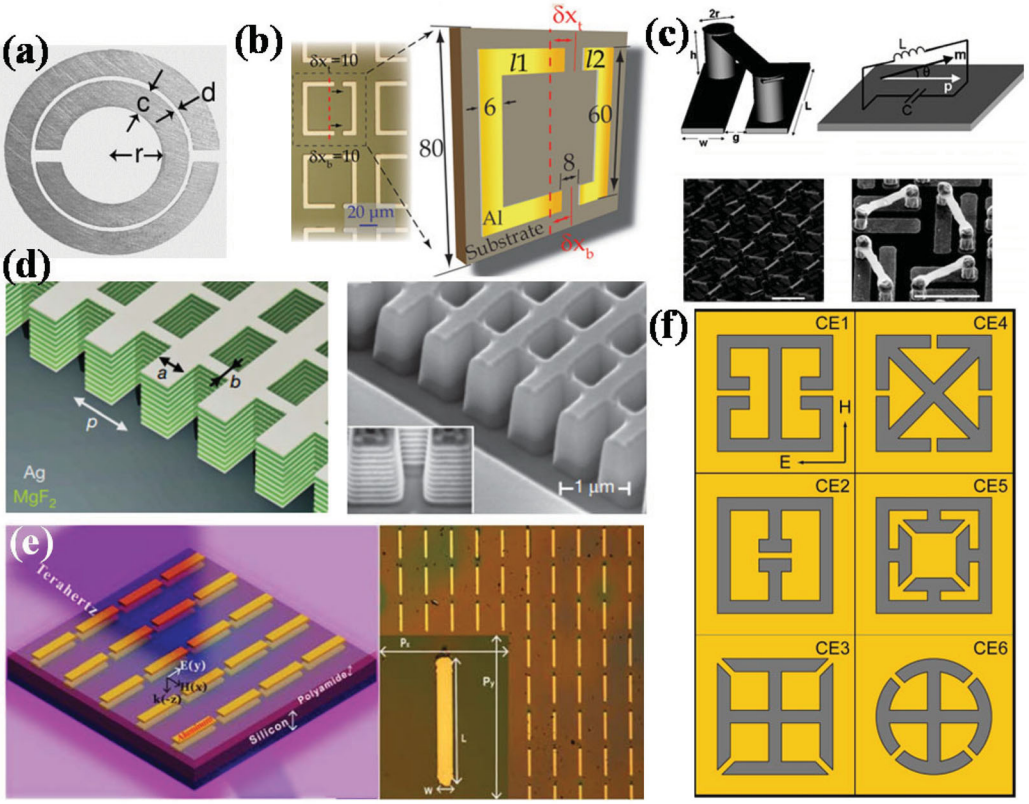

Figure 2. The proposed diversified metamaterial configurations. They are (a) periodic SRR,[59] (b) asymmetric SRR,[61] (c) chiral-shaped metamaterial,[62] (d) three-dimensional stacked metamaterial,[63] (e) line segment-shaped metamaterial,[64] and (f) and complementary electric SRR.[65]

2.3. Configurations

In the past decade, the reconfigurable metamaterials have attracted great attention from researchers for their extraordinary and excellent optical properties, and their abilities to manipulate the propagation of electromagnetic waves. Along with the rapid development of micro-fabrication technologies, the realization of typical reconfigurable metamaterial devices has become mature. Most of reconfigurable metamaterials reported in literatures are based on periodic resonator arrays on semiconductor substrates, such as periodic SRR,[59] asymmetric SRR,[60] chiral-shaped metamaterial,[61] three-dimensional stacked metamaterial,[62] line segment-shaped metamaterial,[63] and complementary electric SRR[64] as shown in Figure 2. The metamaterial configurations can be designed to possess different electromagnetic properties, e.g. the electromagnetic response of metallic configuration generates from the oscillating free electron coupling with incident wave that generates from the and that of all-dielectric configuration generates from the dipole or quadrupole coupling with incident wave.

In 2000, Smith et al. demonstrated the periodic metamaterial structure composed of SRR array to perform negative permeability as shown in Figure 2(*a*),[59] which verified the left-handed materials proposed by Veselago in 1968.[61] By splitting the ring of SRR, where the capacitor generated from the split gap and the inductor formed by the metallic ring interactively create an inductance–capacitance (LC) resonance. SRR configuration usually exhibits a local enhancement of electromagnetic field to be a suitable candidate of metamaterial unit cell for diversified micro-optical devices. When the SRR array is asymmetrical, there can induce some resonance modes not found

in the symmetric structure, such as Fano resonance as shown in Figure 2(*b*). This asymmetric SRR can generate a narrowband resonance with a high Q-factor, which can be applied in high-sensitive biosensors and chemical sensors applications.[61] A chiral-shaped metamaterial shows chirality generated from the metal wires and the inclined connection structure between metal wires as shown in Figure 2(*c*).[62] This chiral-shaped metamaterial is equivalent to a micro-LC circuit formed by a vertical current loop. The oscillating current flows through the metal wires stimulated by the induced electric field within the split gap and magnetic field perpendicular to the current loop. It generates a strong coupling electromagnetic resonance. This chiral-shaped metamaterial can be considered as a combination of electric and magnetic dipoles. The strong chiral behavior can be expected and the polarization rotation can be equivalently realized by the broken metamaterial symmetry. Figure 2(*d*) shows the three-dimensional stacked metamaterial composed of metal-insulator-metal (MIM) layers. This stacked multi-layers exhibits strong induced magnetic coupling effect between adjacent layers through cascade each other, and the adjacent LC resonators generate broadband and low loss negative refractive index characteristics through the mutual inductance coupling tightly.[63] Due to the cancellation of antisymmetric current through the metal thin-film, the central current flow is effectively offset and the optical loss is further reduced. It is conducive to the construction of functional metamaterial devices with low optical loss. When the normal incident electromagnetic wave shines on the metamaterial surface, the electromagnetic resonant modes are affected by the structural symmetry. Compared to the typical SRR configuration, the line segment-shaped metamaterial usually shows wide bandwidth of resonance. The introduction of two stacked layers facilitates the limit of electromagnetic energy to deep sub-wavelength range, and then generates a Fano resonance. This Fano resonance can be tuned by changing the thickness of dielectric layer between metamaterials as shown in Figure 2(*e*).[64] Figure 2(*f*) shows the complementary electric SRR structures, which metal patterns are replaced by the perforated regions compared with the typical electric SRR structures. These kind of complementary electric SRR structures are named as "complementary metamaterials." When the incident electromagnetic wave is perpendicular to the metamaterial with and without complementary structure, the electromagnetic field of transmission coefficient follows the Babinet theory: $t(\omega) + t_c(\omega)=1$.[65] Therefore, the perforated region of complementary metamaterial has higher surface current density due to there has a larger local electric field within the complementary metamaterial structure. Similarly, the enhanced local electric field within the gap of metamaterial structure is corresponding to the region of high surface current density in the complementary metamaterial structure.[65]

2.4. Tuning mechanisms

Metamaterial has greatly promoted the innovation and development of photoelectric integration technology. However, when the metamaterial structures are fabricated on rigid and rough substrates, their geometry sizes, shapes, and patterns cannot be changed. It means the electromagnetic characteristics of metamaterials cannot be controlled. That will hinder the flexibility and applicability of metamaterials. If the metamaterial configurations can be manipulated or changed by driving a voltage or other ways, the corresponding resonance of metamaterial could be tuned actively. To date, the common actively tuning methods of metamaterials are included but not limited the electrical tuning, liquid crystal tuning, optical tuning, electromechanical tuning, etc.[36,66–71]

Figure 3(*a*) shows the metamaterial fabricated on a Schottky junction formed by metal and n-GaAs materials. By driving a bias voltage on electrode pads of metamaterial, the injection and depletion of carriers within Schottky junction can be controlled. Thus, the manipulation of amplitude and frequency of incident THz wave can be tuned by electrical tuning method.[36] Figure 3(*b*) shows another electrical control approach. The resonant frequency of metamaterial

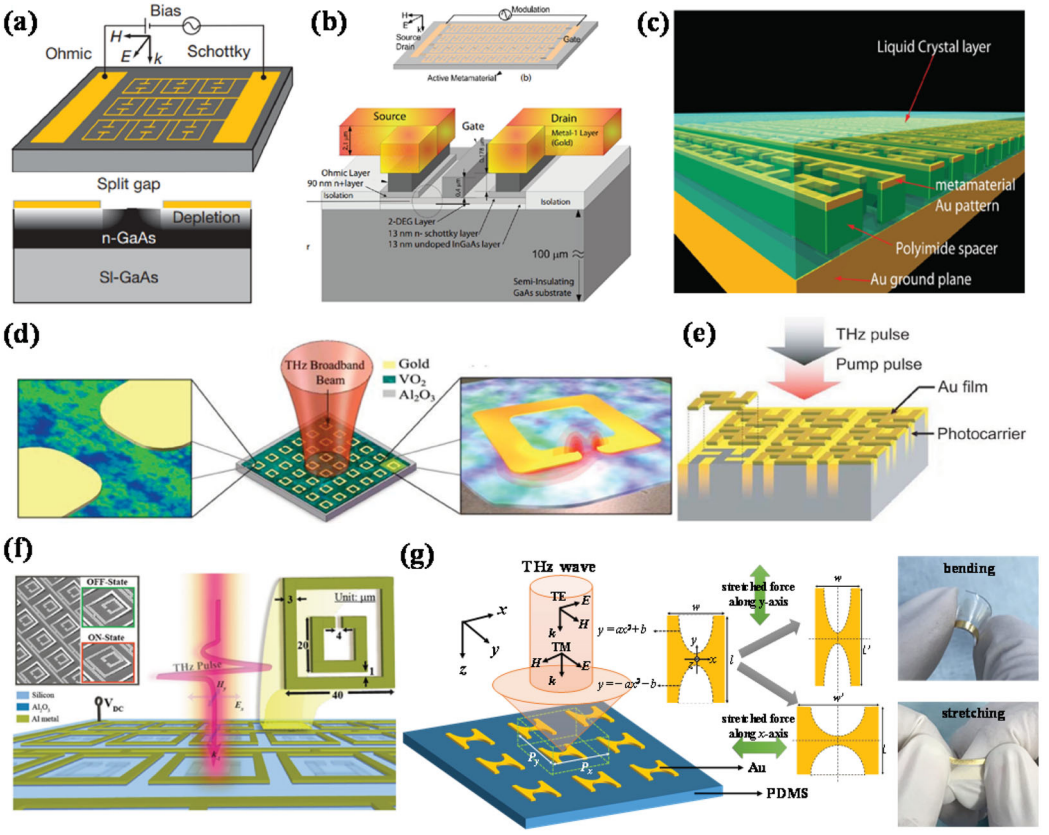

Figure 3. Tuning mechanisms of reconfiguration metamaterials. They are (a) and (b) electrical tuning,[36,66] (c) liquid crystal tuning,[67] (d) and (e) optical tuning,[68,69] (f) and (g) electromechanical tuning.[70,71]

can be tuned by switching on and off states of transistor.[66] The use of electrical tuning mechanism is precise but the tuning range is limited. In Figure 3(*c*), metamaterial surface is covered with a liquid crystal layer. The use of liquid crystal material is an extra implantation method for changing the metamaterial resonance. The electric field of incident THz wave is used to control the direction of liquid crystal monomer and then the resonant characteristic of metamaterial can be tuned.[67] However, the response time is fast using electrical tuning mechanism compared with the use of liquid crystal tuning.

The modulation of resonant frequency can be realized by changing the conductivity of metamaterial dielectric layer, e.g. vanadium dioxide (VO_2), which is sensitive to the surrounding temperature. When the incident light shines on metamaterial surface, VO_2 will absorb the energy of incident light and then increase the surrounding temperature. Therefore, the resonant frequency of metamaterial can be tuned by changing the power of incident light as shown in Figure 3(*d*).[68] Another optical tuning method is used the photogenic carriers generated from the semiconductor substrate. When the incident light is pumped with different powers, the photocarriers are generated to perform the active tuning of resonance as shown in Figure 3(*e*).[69] It is available to regard the optical tuning method that is more precise in the microscale metamaterial, but it is hard to achieve large tuning range. The electromechanical tuning is an alternative candidate for actively reconfigurable metamaterial. In Figure 3(*f*), the release angle of closed ring resonator (CRR) can be controlled to tune the coupling effect between the CRR and the SRR. The signal of resonance can be switched on and off states for achieving a stealth effect.[70] Figure 3(*g*) shows a stretchable parabolic-shaped metamaterial (PSM) coated onto PDMS substrate. By stretching the PSM device

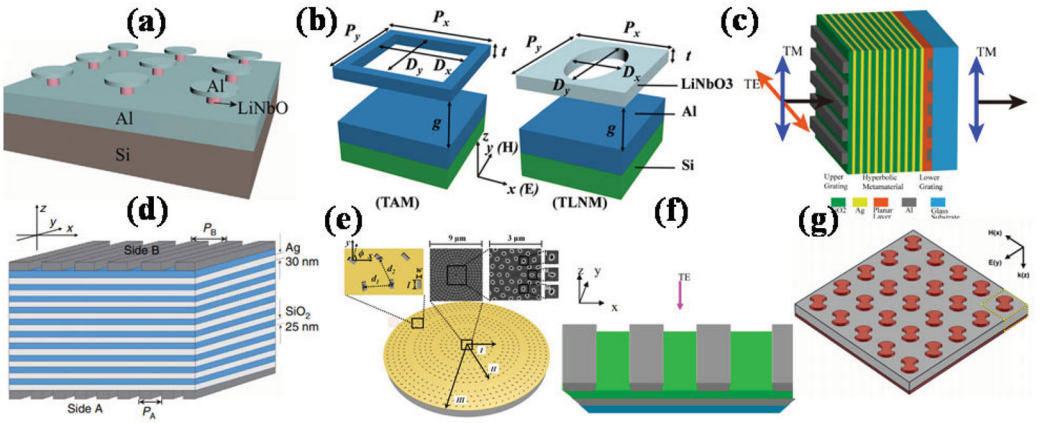

Figure 4. Reconfigurable visible metamaterials for (a) absorber,[79] (b) filter,[80] (c and d) polarizer,[81,82] (e) sensor,[83] (f) switch,[84] and (g) resonator[72] applications.

along different directions, the polarization states and resonances can be changed.[71] These different strain forces applied on PSM are regarded as inputs to reshape the metamaterial configuration, and then tune the transmission spectra. The use of electromechanical tuning method maybe not enough precise compared to above-mentioned methods, but the advantages are applicable to have larger tuning range and cost-effective.

3. Reconfigurable metamaterials in electromagnetic spectra

The developments of reconfigurable metamaterials arise the new or multifunctional optoelectronic devices, which span the whole electromagnetic spectra from visible, IR to THz frequency ranges. This session introduces the applications of reconfigurable metamaterials in the different spectra ranges.

3.1. Reconfigurable visible metamaterials

Since 2000, there have been reported many visible metamaterials to be used in color filters, resonators, absorbers, and sensors.[72–78] Lin et al. proposed four types of suspended nanodisk metasurfaces, which exhibit perfect absorption characteristics with ultrabroad tuning range of resonance spanning the whole visible spectra range and narrower bandwidth as shown in Figure 4(*a*).[79] The same research group also demonstrated two designs of high-efficiency reconfigurable color filter based on suspended rectangular Al and elliptical lithium niobate ($LiNbO_3$) metasurfaces on Si substrate coated with an Al mirror layer atop as shown in Figure 4(*b*).[80] Zhang et al. proposed multilayer gratings by using superimposed metamaterial/metal/dielectric thin-films for hyperbolic spatial frequency filtering. This design performs the high extinction ratio of polarization characteristic in the visible light as shown in Figure 4(*c*)[81]. Florous et al. simulated a heterostructure photonic crystal based on metal nanowires with ultra-low refractive index as shown in Figure 4(*d*)). The results exhibit this heterostructure photonic crystal is wavelength selective and thermal insensitive with low transmission loss.[82] Mehmood et al. demonstrated an ultrathin multifocal optical vortex with different topological charges in each focal plane. These nanopores are bipolar and the polarity of metal materials can be changed by tuning the helicity of incident visible light. Therefore, the detection of the metal polarity is equivalent to the description of incident light as shown in Figure 4(*e*).[83] Zhang et al. proposed a kind of MIM-based Au grating nanostructures to realize the perfect visible light absorption and tunable optical switch as shown in Figure 4(*f*).[84] In Figure 4(*g*), Tuan et al. proposed a broadband metamaterial based on

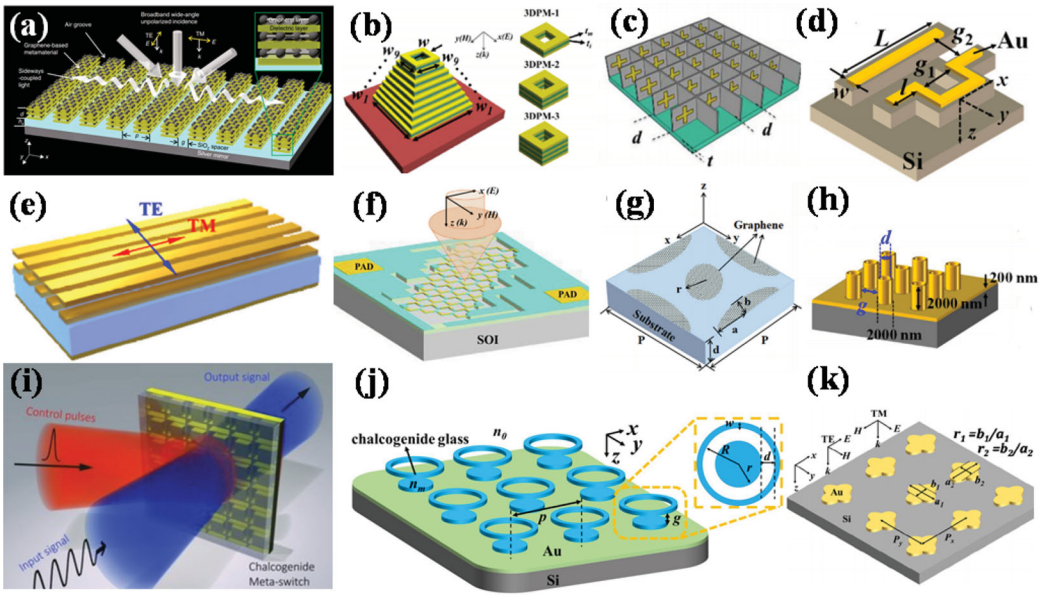

Figure 5. Reconfigurable metamaterials in IR spectrum range for (a and b) absorbers,[73,74] (c and d) polarizers,[75,76], (e and f) filters,[77,78] (g and h) sensors,[85,86] and (i and j) switches[87–89] applications.

MIM configuration to realize a non-polarized resonator.[72] These results provide the development of metamaterial progress in the visible spectrum range.

3.2. Reconfigurable IR metamaterials

In 2019, Han Lin et al. demonstrated 85% absorption characteristic using IR metamaterial composed of 90 nm thick graphene as shown in Figure 5(*a*).[73] It verified that the proposed device could achieve a maximum IR broadband absorption within the range of 60 incident angle. This study provides an approach of metamaterial for the use of IR absorber. In 2020, Lin et al. proposed a tunable three-dimensional pyramid metamaterial with broad absorption bandwidth and maximum absorption intensity of 99% for perfect IR absorber with broad bandwidth as shown in Figure 5(*b*).[74] Campione et al. presented a three-dimensional vertically intersecting dipole array, which performed a higher polarization ratio and bandwidth compared with linear polarimeter and two-dimensional linear dipole array in the IR wavelength range as shown in Figure 5(*c*).[75] This study provides an approach of metamaterial for the use of IR polarizer. Lin et al. showed three types of polarization-sensitive infrared metamaterials with serpentine-shaped Au nanostructures. They exhibit the multifunctionalities of polarization switching and single-/dual-band switching as shown in Figure 5(*d*).[76] The same research group also demonstrated two kinds of plasma metamaterial IR filters, which composed of metal nanogratings on SiO_2 layer with a tuning wavelength range of 2.4 μm as shown in Figure 5(*e*).[77] The IR incident wave can be tuned by changing the vertical distance between top and bottom metal nanogratings using MEMES technique. The IR incident wave can also be tuned horizontally using electrothermal force to change the gap between metamaterials as shown in in Figure 5 (*f*).[78] Liang et al. designed an IR graphene-refractive index metasensor. It is insensitive to the polarization light with wide incident angle and has good angular polarization tolerance as shown in Figure 5(*g*).[85] In 2019, Lin et al. proposed four designs of ultrasensitive IR sensors. They are composed of MIM nanostructures with a maximum Q-Factor of 47 as shown in Figure 5(*h*).[86] As shown in Figure 5(*i*), Gholipour

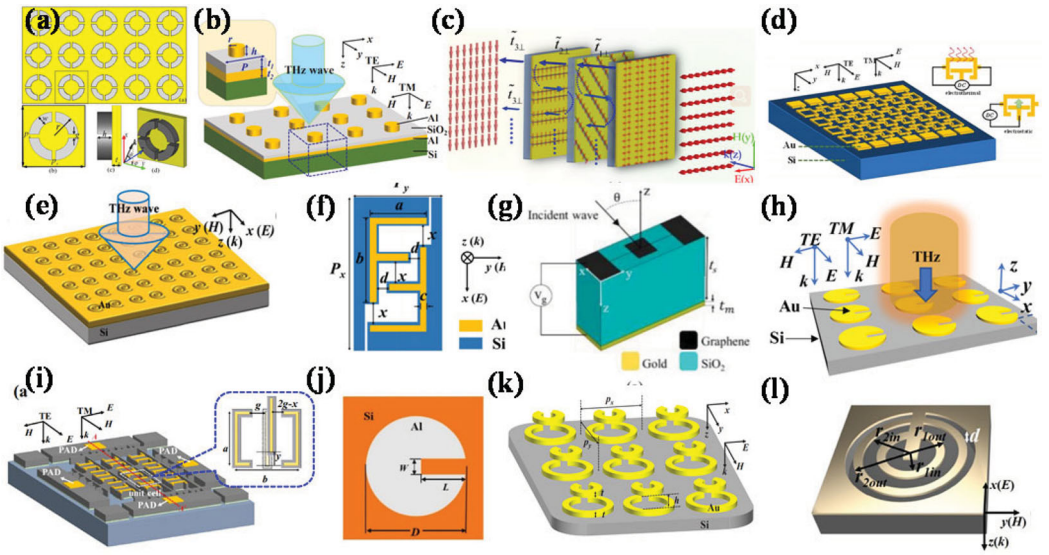

Figure 6. Reconfigurable metamaterials in THz spectrum range for (a and b) absorbers,[90,91] (c and d) polarizers,[75,92] (e and f) filters,[93,94] (g and h) sensors,[85,95] and (i–l) switches[96–99] applications.

et al. demonstrated an metamaterials-based optical switch for near to middle IR wavelengths and verified the non-volatile and reversible optical exchange function by repeating the operation cycle of device.[87] For optical IR switch application, Lin et al. proposed a novel IR metamaterial switch using chalcogenide glass material and it can be tuned and switched by single, dual, and triple resonances as shown in Figure 5(*j*).[88] Meanwhile, they also demonstrated the switching function of single-band to dual-band resonances, broad and narrow bandwidths using single ellipse-shape metamaterials and cross ellipse-shape metamaterials as shown in Figure 5(*k*).[89] The above-mentioned are the reconfigurable IR metamaterials for the uses of absorbers, polarizers, filters, sensors, and switches applications.

3.3. Reconfigurable THz metamaterials

Cheng et al. proposed a wide-band THz absorber, which can be used as a THz black body as shown in Figure 6(*a*).[90] The absorptivity of the metamaterial THz absorber is 99.9%. This proposed device has the potential uses in photodetector, thermal imaging, photoelectrochemistry and solar energy harvester applications. Lin et al. proposed an ultra-narrowband THz perfect absorber composed of MIM microstructures. The absorption intensity of proposed device is 99% with an ultra-high Q-factor of 143 as shown in Figure 6(*b*).[91] Figure 6(*c*) shows a three-layered metamaterial to effectively rotate THz wave as a linear polarizer.[75] They also demonstrated a tunable THz chain-link metamaterial to exhibit bidirectional polarization-dependence as shown in Figure 6(*d*).[92] Meanwhile, they proposed and demonstrated two designs of complementary spiral-shape metamaterials with square and hexagonal meta-atom arrangements, which perform the tunable THz filters by applying a DC bias voltage on device as shown in Figure 6(*e*).[93] Figure 6(*f*) shows an asymmetric F-shaped metamaterial composed of Au layers on SOI substrate to realize a tunable THz filter with high full width at half maximum (FWHM) value.[94] In Figure 6(*g*), a metamaterial sensor with a simple design is presented. The strong coupling of surface plasmon resonance and structural resonance of graphene induces a very narrow absorption peak.[85] In the Lin's research group, they proposed a series of THz metamaterial sensors and switches, such as three designs of tunable multi-resonance of THz metamaterials composed of single-, dual-, and triple-split-disk resonators (Figure 6(*h*)),[95] a tunable THz metamaterial with single-band and

dual-band filtering and switching characteristics (Figure 6(*i*)),[96] a multifunctional split-disk resonator THz metamaterial (Figure 6(*j*)),[97] a three-dimensional double split-ring resonators with high tuning range (Figure 6(*k*))[98] and three-coaxial-complementary-SRR metamaterial with single-/dual-band switching tunability (Figure 6(*l*)).[99] The fruitful results provide the reconfigurable THz metamaterials to possess multifunctional characteristics.

4. Emerging applications of reconfigurable metamaterials

In the past decade, metamaterials have diversified many applications along with the rapid development of reconfigurable metamaterials. The current emerging fields are included but not limited the biosensing,[100–111] opto-logic,[112–115] and optical communication[66,116,117] applications. For biosensing application, by reasonably designing the metamaterial structure, the electromagnetic field could be confined within the metamaterial configuration and then enhanced the interaction between the incident electromagnetic wave and the sensing target. The metamaterials are used to enhance the absorption of THz signal, which is regarded as signal amplifier for sensing protein molecules by matching the absorption peak of protein molecules with metamaterial resonance. In addition to the sensing category, the analyte shape is also an important issue to determine the sensing capability.[100] For examples, the typical method of detecting the carbohydrate molecules is used a slot metamaterial antenna array. It can identify various concentrations within the scope of all kinds of carbohydrate molecules. These molecules can be detected effectively by metamaterial antenna to enhance the molecular absorption.[101] The researchers put forward a kind of complementary metamaterials with square crack structures on high-resistance Si substrate. It can detect kanamycin sulfate with the sensitivity of 100 pg/L. This study demonstrated the near field enhancement for the increment of sensitivity significantly owing to the metamaterial strong coupling effect.[102] According to artificial surface plasma excitation, the subwavelength groove array is proposed for optical sensing.[103] The monitoring spectra window is from 0.40 THz to 1.44 THz. It becomes a possible way to detect the substance category and concentration by changing the refractive index of various liquids. Currently, the metamaterial-based biosensors are integrated with microfluidic chips to analyze the bio-specimens.[104–111]

For opto-logic switching application, Kim et al. presented programmable nonvolatile memory components using graphene and ferroelectric crystals and further extended the concept by establishing reconfigurable logic gates in 2016.[116] When there is a single input, the stored data can be kept at room temperature for more than 10 years, which amplitudes, phases and polarization patterns can be clearly distinguished. Lee et al. demonstrated a 1-bit logic device composed of MEMS reconfigurable metamaterial to switch on and off states.[113] To increase the bit rate of logic device, Lin et al. proposed MEMS-based reconfigurable logic metamaterials,[114,115] which corresponding resonance is denoted as signal "1," and that without resonance is denoted as signal "0." These MEMS-based reconfigurable logic metamaterials perform more than 2-bits logic switches.

In 2017, a design of plasmonic nanocavities integrated with a photonic-plasmonic hybrid circuit is applied for the near-field transportation signal in the nanocavity.[116] In 2018, a thin film phase modulator employing organic nonlinear optical molecules is proposed to act as coherent electric field detector for THz communication system.[117] A THz metamaterial based high electron mobility transistor (HEMT) is demonstrated to be capable of modulation depths up to 33% at 0.46 THz with all electrical control, and the modulation of THz radiation is up to 10 MHz.[66] It opens the avenue for metamaterial implanted into transistor fields. In 2020, a reconfigurable THz filter composed of ring-shaped and cross-shaped nanostructures is presented by Lin's research group.[118] It was used to control the output frequency window for an indoor THz wireless communication system, which makes the data rates up to 100 Gb/s more possible. These results pave a way for the metamaterials to be used in the future optical communication with a cost-effective, flexible, and applicable approach.

5. Summary and outlook

The reconfigurable metamaterials have brought up novel ideas and enabled many emerging applications. It is because the passive or active control of reconfigurable metamaterials can further extend their applicability without extra components integrated into the system. To make metamaterials more flexibility and applicability, the choices of substrates, materials, configurations and tuning mechanisms play very important roles. The reconfigurable metamaterials exhibit assuredly unprecedented capabilities in the manipulation of incident electromagnetic wave, e.g. polarization, frequency, amplitude and phase spanned the visible, IR and THz spectra ranges. They allow for the implementations of many traditional optical devices. Therefore, they facilitate some advanced optoelectronic devices and their applications. Although the characterizations of reconfigurable metamaterials are excellent, however, there still has some challenges to compare with the traditional optical devices. For example, metamaterial-based devices are hard to integrate with current IC circuits for the real widespread applications. It hampers the development of metamaterial optics for commercial products. By overcoming this issue, the reconfigurable metamaterials would have many potential opportunities to implant into current optoelectronics, optical communications, data analysis, and fundamental physic studies.

Funding

The authors acknowledge the financial support from National Key Research and Development program of China [2019YFA0705004] and the State Key Laboratory of Optoelectronic Materials and Technologies of Sun Yat-Sen University for the use of experimental equipment.

References

[1] Huang, L.; Chang, C.-C.; Zeng, B.; Nogan, J.; Luo, S.-N.; Taylor, A. J.; Azad, A. K.; Chen, H.-T. Bilayer metasurfaces for duaand broadband optical antireflection. *ACS Photonics.* **2017**, *4*, 2111–2116.

[2] Unlu, M.; Hashemi, M. R.; Berry, C. W.; Li, S.; Yang, S.-H.; Jarrahi, M. Switchable scattering metasurfaces for broadband terahertz modulation. *Sci. Rep.* **2014**, *4*, 5706–5708.

[3] Smith, M.; Malak, S.; Jung, J.; Yoon, Y. J.; Lin, C. H.; Kim, S.; Lee, K. M.; Ma, R.; White, T. J.; Bunning, T. J.; Lin, Z.; Tsukruk, V. V. Robust, uniform, and highly emissive quantum dot–polymer films and patterns using Thiol-Ene chemistry. *ACS Appl. Mater. Interfaces* **2017**, *9*, 17435–17448.

[4] Misra, S.; Li, L.; Jian, J.; Huang, J.; Wang, X.; Zemlyanov, D.; Jang, J.-W.; Ribeiro, F. H.; Wang, H. Tailorable Au nanoparticles embedded in epitaxial TiO2 thin films for tunable optical properties. *ACS Appl. Mater. Interfaces.* **2018**, *10*, 32895–32902.

[5] Wu, D. M.; Solomon, M. L.; Naik, G. V.; García-Etxarri, A.; Lawrence, M.; Salleo, A.; Dionne, J. A. Chemically responsive elastomers exhibiting unity order refractive index modulation. *Adv. Mater.* **2018**, *30*, 1703912.

[6] Chiam, S.-Y.; Singh, R.; Zhang, W.; Bettiol, A. A. Controlling metamaterial resonances via dielectric and aspect ratio effects. *Appl. Phys. Lett.* **2010**, *97*, 191906.

[7] Chowdhury, D. R.; Singh, R.; Reiten, M.; Zhou, J.; Taylor, A. J.; O'Hara, J. F. Tailored resonator coupling for modifying the terahertz metamaterial response. *Opt. Express.* **2011**, *19*, 10679–10685.

[8] Zhu, W. M.; Liu, A. Q.; Zhang, W.; Tao, J. F.; Bourouina, T.; Teng, J. H.; Zhang, X. H.; Wu, Q. Y.; Tanoto, H.; Guo, H. C.; Lo G. Q.; Kwong D. L. Polarization dependent state to polarization independent state change in THz metamaterials. *Appl. Phys. Lett.* **2011**, *99*, 221102.

[9] Li, X.; Yang, T.; Zhu, W.; Li, X. Continuously tunable terahertz metamaterial employing a thermal actuator. *Microsyst. Technol.* **2013**, *19*, 1145–1151.

[10] Li, Q.; Tian, Z.; Zhang, X.; Xu, N.; Singh, R.; Gu, J.; Lv, P.; Luo, L.-B.; Zhang, S.; Han, J.; Zhang, W. Dual control of active graphene–silicon hybrid metamaterial devices. *Carbon.* **2015**, *90*, 146–153.

[11] Al-Naib, I.; Yang, Y.; Dignam, M. M.; Zhang, W.; Singh, R. Ultra-high Q even eigenmode resonance in terahertz metamaterials. *Appl. Phys. Lett.* **2015**, *106*, 011102.

[12] Cong, L.; Srivastava, Y.; Singh, R. Near-field inductive coupling induced polarization control in metasurfaces. *Adv. Opt. Mater.* **2016**, *4*, 848–852.

[13] Gao, X.; Che, W.; Feng, W. Novel non-periodic spoof surface plasmon polaritons with H-shaped cells and its application to high selectivity wideband bandpass filter. *Sci. Rep.* **2018**, *8*, 1–7.
[14] Shih, K.; Pitchappa, P.; Manjappa, M.; Ho, C. P.; Singh, R.; Yang, B.; Singh, N.; Lee, C. Active MEMS metamaterials for THz bandwidth control. *Appl. Phys. Lett.* **2017**, *110*, 161108.
[15] Manukumara, M.; Prakash, P.; Navab, S.; Nan, W; Nikolay, I. Z.; Chengkuo, L.; Ranjan, S. Reconfigurable MEMS Fano metasurfaces with multiple-input-output states for logic operations at terahertz frequencies. *Nat. Commun.* **2018**, *9*, 4056.
[16] Keng-Te, L.; Han, L.; Tieshan, Y.; Lin, K.-T.; Lin, H.; Yang, T.; Jia, B. Structured graphene metamaterial selective absorbers for high efficiency and omnidirectional solar thermal energy conversion. *Nat. Commun.* **2020**, *11*, 1389.
[17] Wang, Q.; Rogers, E. T. F.; Gholipour, B.; Wang, C.-M.; Yuan, G.; Teng, J.; Zheludev, N. I. Optically reconfigurable metasurfaces and photonic devices based on phase change materials. *Nat. Photon.* **2016**, *10*, 60–65. DOI: 10.1038/nphoton.2015.247.
[18] Pitchappa, P.; Kumar, A.; Liang, H.; Prakash, S.; Wang, N.; Bettiol, A. A.; Venkatesan, T.; Lee, C.; Singh, R. Frequency-agile temporal terahertz metamaterials. *Adv. Opt. Mater.* **2020**, *8*, 2000101.
[19] Pitchappa, P.; Manjappa, M.; Ho, C. P.; Singh, R.; Singh, N.; Lee, C. Active control of electromagnetically induced transparency analog in terahertz MEMS metamaterial. *Adv. Opt. Mater.* **2016**, *4*, 541–547.
[20] Manjappa, M.; Srivastava, Y. K.; Cong, L.; Al-Naib, I.; Singh, R. Active photoswitching of sharp *Fano resonances in THz metadevices. *Adv. Mater.* **2017**, *29*, 1603355.
[21] Manjappa, M.; Solanki, A.; Kumar, A.; Sum, T. C.; Singh, R. Solution-processed lead iodide for ultrafast all-optical switching of terahertz photonic devices. *Adv. Mater.* **2019**, *31*, 1901455.
[22] Pitchappa, P.; Kumar, A.; Prakash, S.; Jani, H.; Venkatesan, T.; Singh, R. Chalcogenide phase change material for active terahertz photonics. *Adv. Mater.* **2019**, *31*, 1808157.
[23] Kumar, A.; Solanki, A.; Manjappa, M.; Ramesh, S.; Srivastava, Y. K.; Agarwal, P.; Sum, T. C.; Singh, R. Excitons in 2D perovskites for ultrafast terahertz photonic devices. *Sci. Adv.* **2020**, *6*, eaax8821.
[24] Ou, J.-Y.; Plum, E.; Zhang, J.; Zheludev, N. I. An electromechanically reconfigurable plasmonic metamaterial operating in the near-infrared. *Nat. Nanotechnol.* **2013**, *8*, 252–255.
[25] Srivastava, Y. K.; Manjappa, M.; Cong, L.; Krishnamoorthy, H. N. S.; Savinov, V.; Pitchappa, P.; Singh, R. Superconducting dual-channel photonic switch. *Adv. Mater.* **2018**, *30*, 1801257.
[26] Lim, W. X.; Manjappa, M.; Srivastava, Y. K.; Cong, L.; Kumar, A.; MacDonald, K. F.; Singh, R. Ultrafast all-optical switching of germanium-based flexible metaphotonic devices. *Adv. Mater.* **2018**, *30*, 1705331.
[27] Pitchappa, P.; Manjappa, M.; Krishnamoorthy, H. N. S.; Chang, Y.; Lee, C.; Singh, R. Bidirectional reconfiguration and thermal tuning of microcantilever metamaterial device operating from 77K to 400K. *Appl. Phys. Lett.* **2017**, *111*, 261101.
[28] Manjappa, M.; Srivastava, Y. K.; Solanki, A.; Kumar, A.; Sum, T. C.; Singh, R. Hybrid lead halide perovskites for ultrasensitive photoactive switching in terahertz metamaterial devices. *Adv. Mater.* **2017**, *29*, 1605881.
[29] Pitchappa, P.; Manjappa, M.; Ho, C. P.; Singh, R.; Singh, N.; Lee, C. Active control of electromagnetically induced transparency with dual dark mode excitation pathways using MEMS based tri-atomic metamolecules. *Appl. Phys. Lett.* **2016**, *109*, 211103.
[30] Pitchappa, P.; Ho, C. P.; Cong, L.; Singh, R.; Singh, N.; Lee, C. Reconfigurable digital metamaterial for dynamic switching of terahertz anisotropy. *Adv. Opt. Mater.* **2016**, *4*, 391–398.
[31] Pitchappa, P.; Manjappa, M.; Ho, C. P.; Qian, Y.; Singh, R.; Singh, N.; Lee, C. Active control of near-field coupling in conductively coupled MEMS metamaterial devices. *Appl. Phys. Lett.* **2016**, *108*, 111102.
[32] Pitchappa, P.; Ho, C. P.; Dhakar, L.; Qian, Y.; Singh, N.; Lee, C. Periodic array of subwavelength MEMS cantilevers for dynamic manipulation of terahertz waves. *J. Microelectromech. Syst.* **2015**, *24*, 525–527.
[33] Melik, R.; Unal, E.; Perkgoz, N. K.; Puttlitz, C.; Demir, H. V. Metamaterial-based wireless strain sensors. *Appl. Phys. Lett.* **2009**, *95*, 011106.
[34] Ho, C. P.; Pitchappa, P.; Lin, Y.-S.; Huang, C.-Y.; Kropelnicki, P.; Lee, C. Electrothermally actuated microelectromechanical systems based omega-ring terahertz metamaterial with polarization dependent characteristics. *Appl. Phys. Lett.* **2014**, *104*, 161104.
[35] Tao, H.; Landy, N. I.; Bingham, C. M.; Zhang, X.; Averitt, R. D.; Padilla, W. J. A metamaterial absorber for the terahertz regime: Design, fabrication and characterization. *Opt. Express.* **2008**, *16*, 7181–7188.
[36] Chen, H.-T.; Padilla, W. J.; Zide, J. M. O.; Gossard, A. C.; Taylor, A. J.; Averitt, R. D. Active terahertz metamaterial devices. *Nature* **2006**, *444*, 597–600.
[37] Gu, J.; Singh, R.; Tian, Z.; Cao, W.; Xing, Q.; He, M.; Zhang, J. W.; Han, J.; Chen, H.-T.; Zhang, W. Terahertz superconductor metamaterial. *Appl. Phys. Lett.* **2010**, *97*, 071102.
[38] Su, X.; Ouyang, C.; Xu, N.; Tan, S.; Gu, J.; Tian, Z.; Singh, R.; Zhang, S.; Yan, F.; Han, J.; Zhang W. Dynamic mode coupling in terahertz metamaterials. *Sci. Rep.* **2015**, *5*, 10823.

[39] Dayal, G.; Ramakrishna, S. A. Design of multi-band metamaterial perfect absorbers with stacked metal–dielectric disks. *J. Opt.* **2013**, *15*, 055106.
[40] Chen, H.-T.; O'Hara, J. F.; Azad, A. K.; Taylor, A. J.; Averitt, R. D.; Shrekenhamer, D. B.; Padilla, W. J. Experimental demonstration of frequency-agile terahertz metamaterials. *Nat. Photon.* **2008**, *2*, 295–298.
[41] Katsarakis, N.; Koschny, T.; Kafesaki, M. Electric coupling to the magnetic resonance of split ring resonators. *Appl. Phys. Lett.* **2004**, *84*, 2943–2945.
[42] Choi, M.; Lee, S. H.; Kim, Y.; Kang, S. B.; Shin, J.; Kwak, M. H.; Kang, K.-Y.; Lee, Y.-H.; Park, N.; Min, B. A terahertz metamaterial with unnaturally high refractive index. *Nature.* **2011**, *470*, 369–373.
[43] Shan, Y.; Chen, L.; Shi, C.; Cheng, Z.; Zang, X.; Xu, B.; Zhu, Y. Ultrathin flexible dual band terahertz absorber. *Opt. Commun.* **2015**, *350*, 63–70.
[44] Liu, X.; MacNaughton, S.; Shrekenhamer, D. B.; Tao, H.; Selvarasah, S.; Totachawattana, A.; Averitt, R. D.; Dokmeci, M. R.; Sonkusale, S.; Padilla, W. J. Metamaterials on parylene thin film substrates: Design, fabrication, and characterization at terahertz frequency. *Appl. Phys. Lett.* **2010**, *96*, 011906.
[45] Li, J.; Shah, C. M.; Withayachumnankul, W.; Ung, B. S.-Y.; Mitchell, A.; Sriram, S.; Bhaskaran, M.; Chang, S.; Abbott, D. Mechanically tunable terahertz metamaterials. *Appl. Phys. Lett.* **2013**, *102*, 121101.
[46] Li, J.; Shah, C. M.; Withayachumnankul, W.; Ung, B. S.-Y.; Mitchell, A.; Sriram, S.; Bhaskaran, M.; Chang, S.; Abbott, D. Flexible terahertz metamaterials for dual-axis strain sensing. *Opt. Lett.* **2013**, *38*, 2104–2106.
[47] Zaichun, C.; Rahmani, M.; Yandong, G.; Chong, C. T.; Minghui, H. Realization of variable three-dimensional terahertz metamaterial tubes for passive resonance tunability. *Adv. Mater.* **2012**, *24*, OP143–OP147.
[48] Li, Y.; Huang, Q.; Wang, D. C.; Li, X.; Hong, M. H.; Luo, X. G. Polarization-independent broadband terahertz chiral metamaterials on flexible substrate. *Appl. Phys. A.* **2014**, *115*, 57–62.
[49] Liu, Z.; Huang, C.-Y.; Liu, H.; Zhang, X.; Lee, C. Resonance enhancement of terahertz metamaterials by liquid crystals/indium tin oxide interfaces. *Opt. Express.* **2013**, *21*, 6519–6525.
[50] Singh, R.; Cao, W.; Al-Naib, I.; Cong, L.; Withayachumnankul, W.; Zhang, W. Ultrasensitive terahertz sensing with high-Q Fano resonances in metasurfaces. *Appl. Phys. Lett.* **2014**, *105*, 171101.
[51] Khorshidi, M.; Zafari, S.; Dadashzadeh, G. Increase in terahertz radiation power of plasmonic photoconductive antennas by embedding buried three-stepped rods in electrodes. *Opt. Express.* **2019**, *27*, 22327–22338.
[52] Ahmadivand, A.; Gerislioglu, B.; Tomitaka, A.; Manickam, P.; Kaushik, A.; Bhansali, S.; Nair, M.; Pala, N. Extreme sensitive metasensor for targeted biomarkers identification using colloidal nanoparticles-integrated plasmonic unit cells. *Biomed. Opt. Express.* **2018**, *9*, 373–386.
[53] Shen, N.-H.; Kafesaki, M.; Koschny, T.; Zhang, L.; Economou, E. N.; Soukoulis, C. M. Broadband blueshift tunable metamaterials and dualband switches. *Phys. Rev. B.* **2009**, *79*, 161102.
[54] Kong, X. R.; Zhang, H. F.; Dao, R. N. A tunable ultra-broadband THz absorber based on a phase change material. *J. Electron. Mater.* **2019**, *48*, 7040–7047.
[55] Chen, H.-T.; Yang, H.; Singh, R.; O'Hara, J. F.; Azad, A. K.; Trugman, S. A.; Jia, Q. X.; Taylor, A. J. Tuning the resonance in high-temperature superconducting terahertz metamaterials. *Phys. Rev. Lett.* **2010**, *105*, 247402.
[56] Chen, H.-T.; Zhou, J.; O'Hara, J. F.; Chen, F.; Azad, A. K.; Taylor, A. J. Antireflection coating using metamaterials and identification of its mechanism. *Phys. Rev. Lett.* **2010**, *105*, 073901.
[57] Ahmadivand, A.; Sinha, R.; Karabiyik, M.; Vabbina, P. K.; Gerislioglu, B.; Kaya, S.; Pala, N. Tunable THz wave absorption by graphene assisted plasmonic metasurfaces based on metallic split ring resonators. *J. Nanopart. Res.* **2017**, *19*, 3.
[58] Zhu, J.; Li, S.; Deng, L.; Zhang, C.; Yang, Y.; Zhu, H. Broadband tunable terahertz polarization converter based on a sinusoidally slotted graphene metamaterial. *Opt. Mater. Express.* **2018**, *8*, 1164–1173.
[59] Smith, D. R.; Padilla, W. J.; Vier, D. C.; Nemat-Nasser, S. C.; Schultz, S. Composite medium with simultaneously negative permeability and permittivity. *Phys. Rev. Lett.* **2000**, *84*, 4184–4187.
[60] Veselago, V. G. The electrodynamics of substances with simultaneously negative values of ε and μ. *Sov. Phys. Usp.* **1968**, *10*, 509–514.
[61] Cong, L.; Manjappa, M.; Xu, N.; Al-Naib, I.; Zhang, W.; Singh, R. Fano resonances in terahertz metasurfaces: A figure of merit optimization. *Adv. Opt. Mater.* **2015**, *3*, 1537–1543.
[62] Zhang, S.; Park, Y.-S.; Li, J. S.; Lu, X. C.; Zhang, W. L.; Zhang, X. Negative refractive index in chiral metamaterials. *Phys. Rev. Lett.* **2009**, *102*, 023901.
[63] Valentine, J.; Zhang, S.; Zentgraf, T.; Ulin-Avila, E.; Genov, D. A.; Bartal, G.; Zhang, X. Three-dimensional optical metamaterial with a negative refractive index. *Nature.* **2008**, *455*, 376–379.
[64] Karmakar, S.; Banerjee, S.; Kumar, D.; Kamble, G.; Varshney, R. K.; Roy Chowdhury, D. Deepsubwavelength couplinginduced *Fano resonances in symmetric terahertz metamaterials. **Phys. Status Solidi RRL* **2019**, *13*, 1900310.
[65] Chen, H.-T.; O'Hara, J. F.; Taylor, A. J.; Averitt, R. D.; Highstrete, C.; Lee, M.; Padilla, W. J. Complementary planar terahertz metamaterials. *Opt. Express.* **2007**, *15*, 1084–1095.

[66] Shrekenhamer, D.; Rout, S.; Strikwerda, A. C.; Bingham, C.; Averitt, R. D.; Sonkusale, S.; Padilla, W. J. High speed terahertz modulation from metamaterials with embedded high electron mobility transistors. *Opt. Express.* **2011**, *19*, 9968–9975.
[67] Savo, S.; Shrekenhamer, D.; Padilla, W. J. Liquid crystal metamaterial absorber spatial light modulator for THz applications. *Adv. Opt. Mater.* **2014**, *2*, 275–279. DOI: 10.1002/adom.201300384.
[68] Driscoll, T.; Palit, S.; Qazilbash, M. M.; Brehm, M.; Keilmann, F.; Chae, B. G.; Yun, S.-J.; Kim, H. T.; Cho, S. Y.; Jokerst, N. M.; Smith, D. R.; Basov, D. N. Dynamic tuning of an infrared hybridmetamaterial resonance using vanadium dioxide. *Appl. Phys. Lett.* **2008**, *93*, 024101.
[69] Kanda, N.; Konishi, K.; KuwataGonokami, M. Light-induced terahertz optical activity . *Opt. Lett.* **2009**, *34*, 3000–3002.
[70] Manjappa, M.; Pitchappa, P.; Wang, N.; Lee, C.; Singh, R. Active control of resonant cloaking in a terahertz MEMS metamaterial. *Adv. Opt. Mater.* **2018**, *6*, 1800141.
[71] Xu, Z.; Lin, Y. S. A stretchable terahertz parabolic-shaped metamaterial. *Adv. Opt. Mater.* **2019**, *7*, 1900379.
[72] Tran, S.; Nguyen, T. Numerical study of an efficient broadband metamaterial absorber in visible light region. *IEEE Photon. J.* **2019**, *11*, 4600810.
[73] Lin, H.; Sturmberg, B. C. P.; Lin, K. T.; Yang, Y. Y.; Zheng, X. R.; Chong, T. K.; de Sterke, C. M.; Jia, B. H. A 90nm thick graphene metamaterial for strong and extremely broadband absorption of unpolarized light. *Nat. Photonics.* **2019**, *13*, 270–276.
[74] Huang, W.; Xu, R.; Lin, Y.-S.; Chen, C.-H. Three-dimensional pyramid metamaterial with tunable broad absorption bandwidth. *AIP Adv.* **2020**, *10*, 035125.
[75] Campione, S.; Burckel, D. B. Vertically oriented metamaterial broadband linear polarizer. *Electron. Lett.* **2018**, *54*, 584–585.
[76] Wen, Y.; Liang, Z.; Lin, Y.-S.; Chen, C.-H. Active modulation of polarization-sensitive infrared metamaterial. *Opt. Commun.* **2020**, *463*, 125489.
[77] Liang, Z.; Wen, Y.; Zhang, Z.; Liang, Z.; Xu, Z.; Lin, Y.-S.; et al. Plasmonic metamaterial using metalinsulatormetal nanogratings for highsensitive refraction index sensor. *Results Phys.* **2019**, *15*, 102602.
[78] Mo, Y.; Zhong, J.; Lin, Y. S. Tunable chevron-shaped infrared metamaterial. *Mater. Lett.* **2020**, *263*, 127291.
[79] Dai, J.; Xu, R.; Lin, Y.-S.; Chen, C.-H. Tunable electromagnetic characteristics of suspended nanodisk metasurface. *Opt. Laser Technol.* **2020**, *128*, 106214.
[80] Lin, Y.-S.; Dai, J.; Zeng, Z.; Yang, B.-R. Metasurface color filters using Aluminum and Lithium Niobate configurations. *Nanoscale Res. Lett.* **2020**, *15*, 77.
[81] Zhang, W.; Tan, X.; Wu, N.; Li, W.; Jiao, Q.; Yang, S. Broad visible spectral subwavelength polarizer with high extinction ratio using hyperbolic metamaterial. *Opt. Express.* **2019**, *27*, 18399–18409.
[82] Florous, N.; Saitoh, K.; Koshiba, M.; Skorobogatiy, M. Low-temperature-sensitivity heterostructure photonic-crystal wavelength-selective filter based on ultralow-refractive-index metamaterials. *Appl. Phys. Lett.* **2006**, *88*, 121107.
[83] Mehmood, M. Q.; Mei, S.; Hussain, S.; Huang, K.; Siew, S. Y.; Zhang, L.; Zhang, T.; Ling, X.; Liu, H.; Teng, J.; Danner A.; Zhang, S.; Qiu, C. W. Visible-frequency metasurface for structuring and spatially multiplexing optical vortices. *Adv. Mater.* **2016**, *28*, 2533–2539.
[84] Zhang, L.; Wang, Y.; Zhou, L.; Chen, F. Tunable perfect absorber based on gold grating including phase-changing material in visible range. *Appl. Phys. A.* **2019**, *125*, 368.
[85] Liang, C. P.; Niu, G.; Chen, X. F.; Zhou, Z. G.; Yi, Z.; Ye, X.; Duan, T.; Yi, Y.; Xiao, S. Y. Tunable triple-band graphene refractive index sensor with good anglepolarization tolerance. *Opt. Commun.* **2019**, *436*, 57–62.
[86] Luo, J.; Lin, Y. S. High-efficiency of infrared absorption by using composited metamaterial nanotubes. *Appl. Phys. Lett.* **2019**, *114*, 051601.
[87] Gholipour, B.; Zhang, J.; MacDonald, K. F.; Hewak, D. W.; Zheludev, N. I. An all-optical, non-volatile, bidirectional, phase-change meta-switch. *Adv. Mater.* **2013**, *25*, 3050–3054.
[88] Xu, Z.; Xu, R.; Sha, J.; Zhang, B.; Tong, Y.; Lin, Y.-S. Infrared metamaterial absorber by using chalcogenide glass material with a cyclic ringdisk structure. *OSA Continuum.* **2018**, *1*, 573–580.
[89] Liang, Z.; Liu, P.; Lin, Z.; Zhang, X.; Zhang, Z.; Lin, Y.-S. Electromagnetic responses of symmetrical and asymmetrical infrared ellipse-shape metamaterials. *OSA Continuum.* **2019**, *2*, 2153–2161.
[90] Cheng, Y.; Du, C. Broadband plasmonic absorber based on all silicon nanostructure resonators in visible region. *Opt. Mater.* **2019**, *98*, 109441.
[91] Xu, R.; Liu, X.; Lin, Y. S. Tunable ultra-narrowband terahertz perfect absorber by using metalinsulator-metal microstructures. *Results Phys.* **2019**, *13*, 102176.
[92] Liu, P.; Liang, Z.; Lin, Z.; Xu, Z.; Xu, R.; Yao, D.; Lin, Y.-S. Actively tunable terahertz chain-link metamaterial with bidirectional polarization-dependent characteristic. *Sci. Rep.* **2019**, *9*, 9917.

[93] Cheng, S.; Xu, Z.; Yao, D.; Zhang, X.; Zhang, Z.; Lin, Y.-S. Electromagnetically induced transparency interahertz complementary spiral-shape metamaterials. *OSA Continuum.* **2019**, *2*, 2137–2144.
[94] Lin, Z.; Xu, Z.; Liu, P.; Liang, Z.; Lin, Y.-S. Polarization-sensitive terahertz resonator using asymmetrical F-shaped metamaterial. *Opt. Laser Technol.* **2020**, *121*, 105826.
[95] Zheng, D.; Hu, X.; Lin, Y.-S.; Chen, C.-H. Tunable multi-resonance of terahertz metamaterial using split-disk resonators. *AIP Adv.* **2020**, *10*, 025108.
[96] Hu, X.; Zheng, D.; Lin, Y. S. Actively tunable terahertz metamaterial with single-band and dual-band switching characteristic. *Appl. Phys. A.* **2020**, *126*, 110.
[97] Lin, Y.-S.; Yan, K.; Yao, D.; Yu, Y.; et al. Investigation of electromagnetic response of terahertz metamaterial by using split-disk resonator. *Opt. Laser Technol.* **2019**, *111*, 509–514.
[98] Lin, Y.-S.; Liao, S. Q.; Liu, X. Y.; Tong, Y. L.; Xu, Z. F.; Xu, R. J.; Yao, D. Y.; Yu, Y. B. Tunable terahertz metamaterial by using three-dimensional double split-ring resonators. *Opt. Laser Technol.* **2019**, *112*, 215–221.
[99] Ou, H.; Lu, F.; Liao, Y.; Zhu, F.; Lin, Y.-S. Tunable terahertz metamaterial for high-efficiency switch application. *Results Phys.* **2020**, *16*, 102897.
[100] Park, S. J.; Jun, S. W.; Kim, A. R.; Ahn, Y. H. Terahertz metamaterial sensing on polystyrene microbeads: Shape dependence. *Opt. Mater. Express.* **2015**, *5*, 2150–2155.
[101] Lee, D.-K.; Kang, J.-H.; Lee, J.-S.; Kim, H.-S.; Kim, C.; Hun Kim, J.; Lee, T.; Son, J.-H.; Park, Q.-H.; Seo, M. Highly sensitive and selective sugar detection by terahertz nanoantennas. *Sci. Rep.* **2015**, *5*, 1–7.
[102] Xie, L. J.; Gao, W. L.; Shu, J.; Ying, Y. B.; Kono, J. C. Extraordinary sensitivity enhancement by metasurfaces in terahertz detection of antibiotics. *Sci. Rep.* **2015**, *5*, 8671–8674.
[103] Ng, B.; Hanham, S. M.; Wu, J.; Fernández-Domínguez, A. I.; Klein, N.; Liew, Y. F.; Breese, M. B. H.; Hong, M.; Maier, S. A. Broadband terahertz sensing on spoof plasmon surfaces. *ACS Photonics.* **2014**, *1*, 1059–1067.
[104] Tao, H.; Chieffo, L. R.; Brenckle, M. A.; Siebert, S. M.; Liu, M.; Strikwerda, A. C.; Fan, K.; Kaplan, D. L.; Zhang, X.; Averitt, R. D.; Omenetto F. G. Metamaterials on paper as a sensing platform. *Adv. Mater.* **2011**, *23*, 3197–3201.
[105] Bui, T. S.; Dao, T. D.; Dang, L. H.; Vu, L. D.; Ohi, A.; Nabatame, T.; Lee, YPak.; Nagao, T.; Hoang, C. V. Metamaterial-enhanced vibrational absorption spectroscopy for the detection of protein molecules. *Sci. Rep.* **2016**, *6*, 32123.
[106] Wu, X.; Quan, B.; Pan, X.; Xu, X.; Lu, X.; Gu, C.; Wang, L. Alkanethiol-functionalized terahertz metamaterial as label-free, highly-sensitive and specific biosensor. *Biosens. Bioelectron.* **2013**, *42*, 626–631.
[107] Zhang, C.; Liang, L.; Ding, L.; Jin, B.; Hou, Y.; Li, C.; Jiang, L.; Liu, W.; Hu, W.; Lu, Y.; Kang, L.; Xu W.; Chen J.; Wu, P. Labelfree measurements on cell apoptosis using a terahertz metamaterialbased biosensor. *Appl. Phys. Lett.* **2016**, *108*, 241105.
[108] Miyamaru, F.; Hattori, K.; Shiraga, K.; Kawashima, S.; Suga, S.; Nishida, T.; Takeda, M. W.; Ogawa, Y. Highly sensitive terahertz sensing of glycerolwater mixtures with metamaterials. *J. Infrared. Milli. Terahz. Waves.* **2014**, *35*, 198–207.
[109] Park, S.; Yoon, S.; Ahn, Y. Dielectric constant measurements of thin films and liquids using terahertz metamaterials. *RSC Adv.* **2016**, *6*, 69381–69386.
[110] Hu, X.; Xu, G.; Wen, L.; Wang, H.; Zhao, Y.; Zhang, Y.; Cumming, D. R. S.; Chen, Q. Metamaterial absorber integrated microfluidic terahertz sensors. *Laser Photonics Rev.* **2016**, *10*, 962–969.
[111] Wu, X.; Pan, X.; Quan, B.; Xu, X.; Gu, C.; Wang, L. Selfreferenced sensing based on terahertz metamaterial for aqueous solutions. *Appl. Phys. Lett.* **2013**, *102*, 151109.
[112] Kim, W. Y.; Kim, H.-D.; Kim, T.-T.; Park, H.-S.; Lee, K.; Choi, H. J.; Lee, S. H.; Son, J.; Park, N.; Min, B. Graphene–ferroelectric metadevices for nonvolatile memory and reconfigurable logicgate operations. *Nat. Commun.* **2016**, *7*, 10426–10429.
[113] Pitchappa, P.; Ho, C. P.; Dhakar, L.; Lee, C. Microelectromechanically reconfigurable interpixelated metamaterial for independent tuning of multiple resonances at terahertz spectral region. *Optica.* **2015**, *2*, 571–578.
[114] Xu, Z.; Lin, Z.; Cheng, S.; Lin, Y.-S. Reconfigurable and tunable terahertz wrench-shape metamaterial performing programmable characteristic. *Opt. Lett.* **2019**, *44*, 3944–3947.
[115] Hu, X.; Lin, Y. S. Programmable terahertz metamaterial with multiple logic characteristics. *Results Phys.* **2020**, *18*, 103267.
[116] Qi, Z.; Hu, G.; Zheng, P.; Su, R.; Shi, W.; Yun, B.; Zhang, R.; Cui, Y. Fano resonances in ultracompact silicon-on-insulator compatible integrated photonic–plasmonic hybrid circuits. *Adv. Opt. Mater.* **2017**, *5*, 1700304.
[117] Benea-Chelmus, I.-C.; Zhu, T.; Settembrini, F. F.; Bonzon, C.; Mavrona, E.; Elder, D. L.; Heni, W.; Leuthold, J.; Dalton, L. R.; Faist, J. Three-dimensional phase modulator at telecom wavelength acting as a terahertz detector with an electro-optic bandwidth of 1.25 terahertz. *ACS Photonics.* **2018**, *5*, 1398–1403.
[118] Yang, W.; Lin, Y. S. Tunable metamaterial filter for optical communication in the terahertz frequency range. *Opt. Express.* **2020**, *28*, 17620–17629.